



Study on the Accumulated Temperature Distribution Model of Snowmelt Flood Magnitude from the Perspective of Ecological Environmental Protection of Mountain Areas

Yang Liu^(**), Xian-Yong Meng^{(**)(***), Zhi-Hui Liu^{(**)(****)†} and Dan-Lin Yu^(*****)}

^{*}School of Resources and Environment Science, Xinjiang University, Urumqi, 830046, China

^{**}Key Laboratory of Oasis Ecology Ministry of Education, Xinjiang University, 830046, China

^{***}Xinjiang Institute of Ecology and Geography, Chinese Academy of Sciences, Urumqi, 830011, China

^{****}Institute of Arid Ecology and Environment, Xinjiang University, Urumqi, 830046, China

^{*****}Department of Earth & Environmental Studies, Montclair State University, Montclair, NJ, 07043, USA

†Corresponding author: Zhi-Hui Liu

Nat. Env. & Poll. Tech.
Website: www.neptjournal.com

Received: 18-5-2015

Accepted: 19-6-2015

Key Words:

Inverse hydrological problem
Flood magnitude
Cropland environment
Accumulated temperature distribution
Accumulated temperature threshold

ABSTRACT

Mountain flood that causes landslide and other geological disasters can damage the fragile ecological environment in mountain areas. In this paper, threshold and distribution model of accumulated temperature based on snowmelt flood magnitude are designed in mountainous watershed. Meanwhile, input data for this model make use of ample reliable data that include remote sensing and so on. In detail, this model simulates the average watershed temperature by using the meteorologic re-analysis data of the National Center for Atmospheric Research and calculates the average snow depth by using hyperspectral remote sensing data. In addition, the model related data comprise long-term observation experiments of the watershed, including the characteristics of accumulated snow and result of correlation between runoff and infiltration in runoff simulation experiment through distributed hydrological models (i.e., Soil and Water Assessment Tool and Distributed Hydrology Soil Vegetation Model). Finally, the average accumulated temperature of the watershed that causes snowmelt flood can be obtained through the aforementioned method, and the characteristics of the accumulated temperature distribution of the watershed area are determined based on the temperature lapse rate. The characteristics of accumulated temperature distribution can provide decision-making reference for monitoring the ecological environment in mountain areas and preventing and reducing disasters.

INTRODUCTION

Snowmelt flood is a flood disaster that often occurs in high-latitude and mountainous areas, such as northeast and north-west China, Russia, north Europe, and North America. Mountain areas are carriers for people to survive, produce and live. Given the mountain area's fragile ecological environment and snowmelt floods, its ecosystem has been damaged seriously. Specifically, landslides, debris flows and floods erode land and vegetation, worsening the ecological environment. Floods also have great influence on the quality of the river water in mountain areas. For example, the sediment concentration in flood reduces both water transparency and photosynthesis of aquatic plants, leading to reduced water productivity, death of aquatic animals due to lack of oxygen, and further deterioration of river water.

Snowmelt flood is divided into plain and mountain types. Flood is dramatically destructive, unexpected, and difficult to be forecasted because of the complex terrain and uneven time-space distribution in the mountain area (Berezowski et al. 2015). Determining the accumulated temperature-

warning threshold in a certain period according to flood magnitude, providing early effective warning information, and determining the snowmelt flood distribution area can better protect the ecological environment in the mountain area (Georgakakos et al. 1984, Montesarchio et al. 2009).

Many domestic and foreign studies have been conducted on flood warning. For example, Gautam et al. (2013) evaluated the rainfall thresholds of flood forecast stations as well as the risk level of main watersheds in Nepal with Hydrologic Engineering Center-River Analysis System (HEC-RAS) model. Sun et al. (2013) studied the sensitivity of surface heat flux and watershed runoff with land surface model (CLM4) in 2012.

The current paper aims to study the snowmelt flood warning. In addition, this study inverses the accumulated temperature threshold of watersheds and the accumulated temperature distribution of melted snow space to provide decision-making support for the protection of the ecological environment and for the prevention of natural disasters in the mountain area.

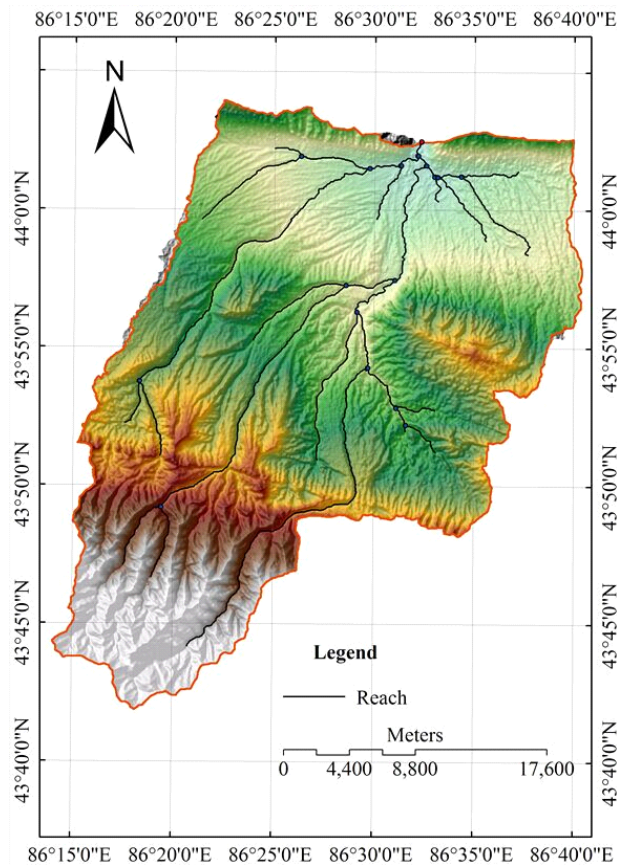


Fig. 1: Location map of the research area.

GENERAL SITUATION OF THE RESEARCH AREA AND DATA PREPARATION

General situation of the research area: This paper selects Juntanghu watershed in Hutubi County on the north face of the Tianshan Mountains in Xinjiang as the research area (Fig. 1). Statistical analysis using geographic information system (GIS) tool shows that the source of the watershed is about 3,400 m high. The height of most parts ranges from 1,000 m to 1,500 m high, with an average height above sea-level of 1,360.31 m. The channels are concentrated at Nazhaer in the low belt, then flow to the plain through Qianshan Hills in the west of Hutubi County, and finally join the Hongshan Reservoir at the exit. The Juntanghu River is about 45.20 km long from the source to the Hongshan Reservoir. The water-collecting area above the Hongshan Reservoir is 833.57 km². The average height of the watershed is 1,503 m. The longitudinal slope of the channel above the junction of two branches in the east and west is 62.5%. The longitudinal slope of the channel from the area below the junction to the Hongshan Reservoir is 52.6%. The average annual runoff is 3.89×10⁸ m³. After reservoir regulation, the water is used by the downstream irrigation area.

Since mid-September, the mountain area in the watershed is covered with snow. With the reduction in air and ground temperatures, the snow will reach the deepest point in January next year. In February, with the rise in air and ground temperatures, the snow begins to melt. In March, the snow begins to melt over a large area. This watershed is closed and complete, with a small catchment area. The watershed has typical characteristics, which comply with the research purpose. In recent years, snowmelt flood has occurred frequently and typically in the watershed. Thus, the watershed is selected for the research.

Data acquisition: The Juntanghu test site has worked for 11 years (2004-2014). Meteorological data depend on the observation of the automatic meteorological station in Juntanghu watershed. Fig. 2 shows that three meteorological stations in the test area have been observed during the snow melting period. Radiation of long and short waves, precipitation, temperature, wind speed, atmospheric pressure, and air humidity is observed.

Each observation point embeds an EM50 observation depth of 5, 15, 20, 25 and 30 cm. The soil temperature and humidity of snow are determined. Permafrost and snow are present at a low-heat conduction. Thus, the heat of the relative net radiation can be ignored when the turbulent exchange of energy is affected. However, when snow layers become thinner, geothermal heat significantly affects snow melting.

INTRODUCTION OF THE MODEL

Accumulated temperature inversion: Heat conduction equation solves the accumulated temperature inversion on the surface area covered with snow. Given that energy transfers from the surface area to the snow and energy is transferred to the snowpack, the core issue of snowmelt flood warning is to calculate the value of accumulated temperature on the surface area covered with snow during this period according to the amount of melted snow. Fig. 3 shows the temperature being transmitted in the snowpack.

If heat transfers from the accumulated snow to the surrounding environment (snowpack and air), then heat transfer is described with Fourier heat transfer equation (Blöschl et al. 1990, 1991, Frey et al. 2015):

$$\rho c \frac{\partial T}{\partial t} = \frac{\partial}{\partial z} \left(\lambda \frac{\partial T}{\partial z} \right), \quad 0 < z \leq L_1, \quad t \geq 0 \quad \dots(1)$$

Where, P is the density of the accumulated snow (kg/m³), t is the heat transfer time(s), c is the specific heat of the accumulated snow(J/kg·K⁻¹), T is the temperature of snow cover on the temperature gradient of the snowpack (K), z is the coordinate axis, and λ is the heat transfer coefficient of the accumulated heat(W/m·K). λ is closely related to P .

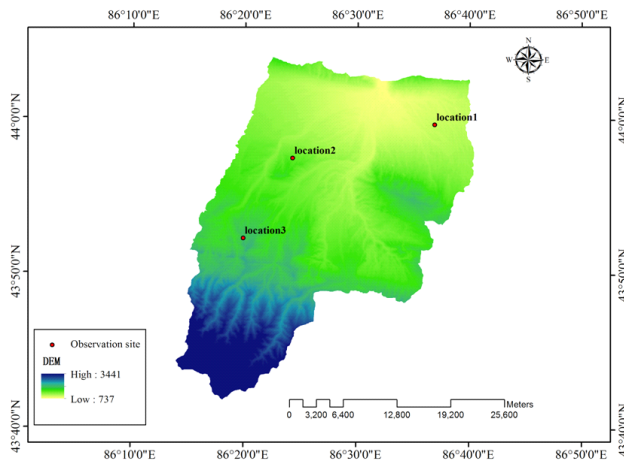


Fig. 2: Location map of the observation site.

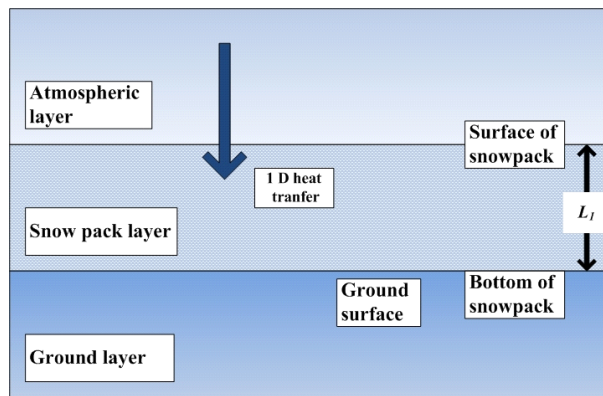


Fig. 3: Sketch map of energy transfer in snow pack.

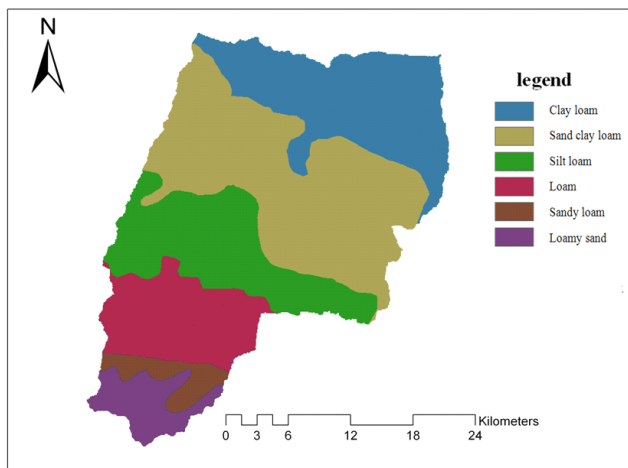


Fig. 4: Soil classification diagram in the research area.

To solve the inverse problem, the boundary condition of temperature T is needed. If the accumulated snow has experienced thermal phase at temperature c and enters the phase-change latent heat stage, the time when the surface

temperature of the snowpack is c is expressed as:

$$T(z,0) = c, \quad 0 < z \leq L_1 \quad \dots(2)$$

Next, the latent heat of the accumulated snow continues to rise and then changes into snow water. The phase-change latent heat Q (MJ/m²) of the accumulated snow melting quantity at time t is the heat flux at the melting period, that is,

$$\lambda \cdot \frac{\partial T}{\partial z}(L_1,t) = Q(t), \quad t \geq 0 \quad \dots(3)$$

If the temperature of the soil surface at the phase-change latent heat stage becomes $f(t)$, the following can be obtained:

$$T(L_1,t) = f(t), \quad t \geq 0 \quad \dots(4)$$

By calculating the equation with boundary conditions (2), (3) and (4) with the Crank-Nicholson implicit difference method of the finite-difference method in partial differential equation, we can determine temperature $T(z,t)$ of each snow cover with time change, including the surface temperature of the accumulated snow $T(0,t)$. The value of the accumulated temperature on the snowpack surface can be calculated according to $T(0,t)$. Numerical simulation is carried out on MATLAB 2015a.

Quantification of heat transfer coefficient of the accumulated snow during the snow melting stage: The snow cover is not a stable solid layer, and the heat transfer coefficient changes with snow density. When the snow changes phase, it melts into water. If the maximum water-holding ability of the snow cover is exceeded, water will run off and take away a considerable amount of heat (Kumar et al. 2015, Sun et al. 2015). Therefore, the heat transfer through the accumulated snow is different from the classical heat transfer problem. To reduce model complexity, effective heat transfer coefficient is defined. Based on the experiment, the relation between snow density and effective heat transfer coefficient is established as follows:

If the density of the accumulated snow is less than 0.45 g·cm⁻³, the heat diffusion coefficient is

$$k_s = 0.307 \rho_s + 1.964 \rho_s^2 \quad \dots(5)$$

If the density is over 0.45 g·cm⁻³, the heat transfer coefficient is:

$$k_s = 2.98 \rho_s - 0.805 \quad \dots(6)$$

In the equation, the unit of k_s is W·m⁻¹·K⁻¹. The density of the accumulated snow is measured with the accumulated snow characteristic tester in the observation area of the experiment. The corresponding heat transfer coefficient can be calculated according to equations (5) and (6).

Heat Calculation at Different Stages During the Snow Melting Process

Sensible heat stage: The sensible heat stage is the initial stage of snow melting. During this stage, the accumulated heat absorbs the heat until the temperature of each layer in the vertical direction reaches 0°C and the vertical layer has no temperature gradient change. To adapt to the snow melting warning, the starting time of warning is set when the accumulated snow has experienced sensible heat stage. The energy change during this stage is not considered.

Phase change stage: After the end of the sensible heat stage, if the accumulated snow continues to absorb heat, it enters the phase change stage. During the phase change stage, the moisture content in the snow rises continuously. When the moisture content exceeds the maximum water-holding capacity of the snow, the snow will run off.

The total amount of snowmelt water during the flood period can be approximately considered as the sum of the flood water and infiltration amount. Thus, the phase change enthalpy (phase-change latent heat) can be calculated according to the principle of water balance.

$$Q_{en} = m_s c_s (T_f - T_i) \quad \dots(7)$$

Where, Q_{en} is the phase change enthalpy, C_s is the specific heat of the snow with value of 33.4 KJ·kg⁻¹·K⁻¹.

Soil properties on the underlying surface of the watershed: The properties of the required soil are determined based on China soil science database and the US soil quantification results of Rawls, Brakensiek and Miller and based on the soil sampling and experimental measurement in the watershed. The results are shown in Fig. 4 and Table 1.

Spatial difference of air temperature: During the snowmelt flood period, the temperature distribution at different altitudes of the watershed is determined according to the air temperatures observed by the meteorological station to determine the distribution of the snow melting intensity.

$$T_i = T_j + a(z_i - z_j) \quad \dots(8)$$

Temperature T_i at i is determined according to temperature T_j at j . The elevations of i and j are different. In the equation, a is the decline rate of the air temperature. Ac-

ording to the experiment and the site observation, the temperature is defined to be 0.0059°C·m⁻¹.

If the air temperature is over 0°C, the accumulated snow begins to melt. T_{aws} is the temperature observed at the elevation of z_{aws} , and T_m is the temperature at the critical elevation of the melting snow. The critical elevation z_m of the melting snow on the elevation belt can be calculated with the following equation:

$$z_m = z_{aws} + a^{-1}(T_{aws} - T_m) \quad \dots(9)$$

MODEL SIMULATION AND RESULTS

In this experiment, two snowmelt floods in Juntanghu watershed were selected for research. The rapidly rising temperature caused the snowmelt flood in Juntanghu watershed. Given that mountainous rivers mainly flow through the gap between mountains, urban and rural residents and fertile fields are mostly distributed in the flood basin along the river coasts. Snowmelt flood covers large areas of grassland and cultivated land. Two snowmelt floods caused about 5 hm² of cultivated land in Hutubi County of Xinjiang to be submerged, leading to crop loss and even failure. About 3 hm² of grassland was destroyed.

Input of the Observation Data in the Model

Determination of the depth of accumulated snow: To monitor the depth of the accumulated snow in a large area, combined with the field observation value of the snow depth, the depth of the accumulated snow was inversed with high spectrum, the accumulated snow depth inversion model during the snowmelt period used 1,456 nm to 1,568 nm and 1,966 nm to 1,992 nm bands, which had significant correlation with the snow depth in the spectral data measured using an Analytical Spectral Devices spectrometer (Xu 2013). The experiment found that the areas near 1,022, 1,241 and 1,492 nm bands were the characteristic absorption valleys of the accumulated snow. The depth of the accumulated snow of each sample was taken as the output to establish the regression model. R² was 0.86 and root mean square error (RMSE) was 0.67, indicating that the regression model could signifi-

Table 1: Soil type and physical parameters.

Soil Type	Void Ratio, η	Effective Void Ratio, θ_e	Soil Matrix Suction at the Moist Frontal Surface, ψ (cm)	Water Power Transmission Coefficient (Permeability Coefficient), K_s (cm/h)
Loamy Sand	0.437(0.363-0.506)	0.401(0.329-0.473)	6.13(1.35-27.94)	2.99
Sandy Loam	0.453(0.351-0.555)	0.412(0.283-0.541)	11.01(2.67-45.47)	1.09
Loam	0.501(0.420-0.582)	0.486(0.394-0.578)	16.68(2.92-95.39)	0.65
Silty Sandy Loam	0.463 (0.375-0.551)	0.434(0.334-0.534)	8.89(1.33-59.38)	0.34
Sandy Clay Loam	0.398(0.332-0.464)	0.330(0.235-0.425)	21.85(4.42-108.0)	0.15
Clay Loam/Loam	0.464(0.409-0.519)	0.309(0.279-0.501)	20.88(4.79-91.10)	0.10

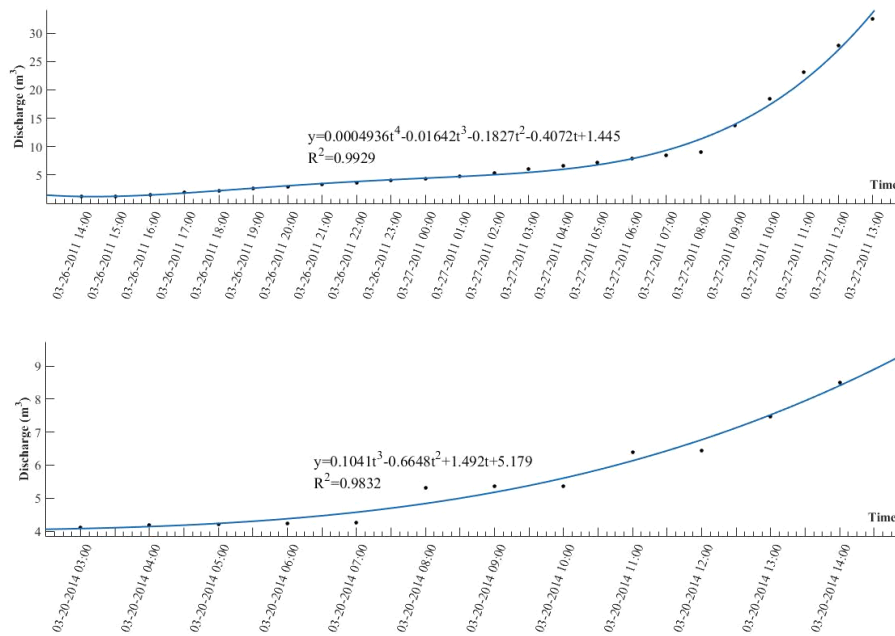


Fig. 5: Flood flow process curve.

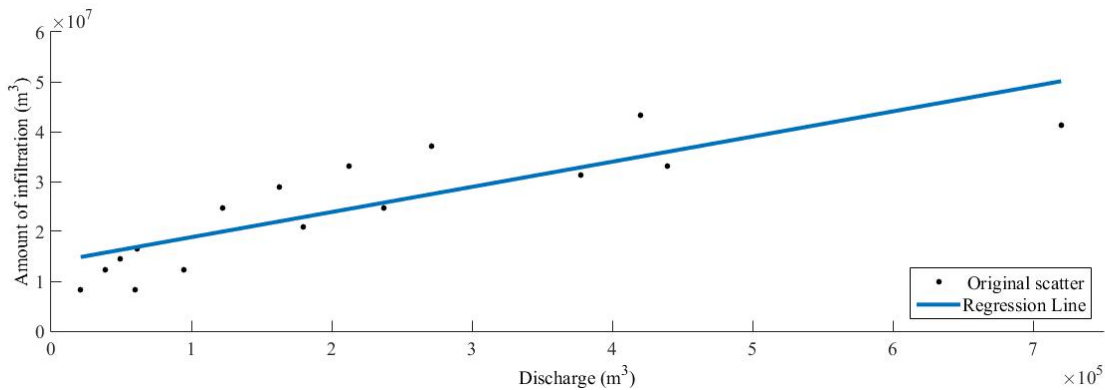


Fig. 6: Original data scatter and regression line.

cantly improve the ability of the hyperspectral data to inverse the depth of the accumulated snow. Table 2 is result and statistical test of snow inversion experiment of snow depth.

Determination of total flow in the flood process: The field observation during the flood season revealed that the areas above observation point 3 had frozen soil, and this part of the watershed area was small (about 8% of the total). Thus, the infiltration of the snowmelt water was not affected by frozen soil, and the form of the runoff yield was runoff yield at natural storage.

The flow process information of two snowmelt floods is shown in Table 3, and the fitting flow process curve is shown

in Fig. 5. For these time series, the corresponding numerical sequence is 1, 2, 3... *N*.

Simulation of the determination of the infiltration amount in the flood period: To reduce the uncertainty of total infiltration amount, the Soil and Water Assessment Tool (SWAT) and Distributed Hydrology Soil Vegetation Model (DHSVM) were applied to simulate the snowmelt flood process experiment in Juntanghu watershed (Xianyong et al. 2013), establish the relevant relationship between the infiltration amount and the runoff, and estimate the cumulative infiltration amount of Juntanghu watershed in a certain period during snow melting, as shown in Fig. 6.

The 95% confidence interval of the estimated regres-

Table 2: Comparison between the snow depth hyperspectral inversion value and the measured values of observation points at 11: 00 on March 12, 2012.

No.	Observation Point	Measured Value (m)	Inversion Value (m)	Relative Error (%)
1	1	0.11	0.095	13.63
2	2	0.156	0.132	15.38
3	3	0.212	0.242	14.15

Table 3: Flow process information of snowmelt flood.

No.	Runoff Yield Form	Observation Period
1	Runoff Yield at Natural Storage	14:00 on Mar. 26, 2011-13:00 on Mar. 27, 2011
2	Runoff Yield at Natural Storage	03:00 on Mar. 20, 2014-17:00 on Mar. 20, 2014

Table 4: Flow process information of snowmelt flood.

No.	Runoff Yield Form	Phase-change Latent Heat of the Snowmelt Water (J)
1	Runoff Yield at Natural Storage	1.67941E+16
2	Runoff Yield at Natural Storage	1.39695E+16

Table 5: Input parameters required for model calculation.

No.	Depth of Accumulated Snow, L_1 (m)	Heat Transfer Coefficient, ($W \cdot m^{-1} \cdot K^{-1}$)
1	0.16	0.22
2	0.22	0.22

Table 6: Input of the boundary value conditions in the equation of the model.

No.	$T(z,0)$ (°C)	$Q(t)$ $0 \leq t \leq 1$	$f(t)$ $0 \leq t \leq 1$
1	0	5421.6t	0
2	0	2923.9t	0

sion coefficient of runoff yield situation at natural storage (1) was in the range of [32.4711, 68.4572]. The scatters in Fig. 6 were the simulation values of SWAT or DHSVM. x was the total simulation flow of an entire flood process, and y was the corresponding total infiltration amount to the simulation.

Inversion of the Accumulated Temperature of the Snow Melting Quantity

Phase-change latent heat of the snow melting quantity: The total snowmelt water of the watershed was the sum of the infiltration amount and floodwater. The total heat quantity of the phase-change latent heat of the accumulated snow

could be calculated according to the total snowmelt water in the watershed. Table 4 is the flow process information of snowmelt flood which shows the phase-change latent heat of the snowmelt.

Inversion of the surface temperature of the accumulated snow during flood period: The accumulated temperature value on the surface of the accumulated snow was inverted based on the total phase-change latent heat of the snowmelt water and the watershed area (Hock 2003). According to the assumption, the temperature of the accumulated snow layer in the sensitive heat phase was 0°C, and the bottom temperature in the phase-change process of the accumulated snow was kept at 0°C. The values were introduced to the boundary value conditions (2) and (4) to inverse the accumulated temperature value on the surface of the snowpack in the watershed before and after the flood ($0 < t < 1$). The boundary value conditions are depicted in Table 5, and the result outputs in Table 6.

The depth of the accumulated snow required by the model was the average snow depth after the hyperspectral remote sensing inversion of observation points 1, 2, and 3. In addition, the density change of the accumulated snow at those three observation points before and after the snow melting process was measured using the accumulated snow characteristic instrument. The heat transfer coefficients could then be obtained based on equations (5) and (6), as depicted in Table 7. The ecological environment in the mountain area is fragile, and the accumulated temperature warning of the snowmelt flood is the focus of the flood prevention work in the mountain area during flood period. Grading the warning according to flood magnitude and taking effective measures to prevent floods in the mountain area are needed to maintain the ecological environment and to protect cultivated land.

STATISTICAL TEST

To test the reliability of the warning model, a statistical test was conducted on the simulated value of the model and measured data. Average relative error was used in the test. The calculation formula is as follows:

$$\text{Average Relative Error} = \frac{\sum_{i=1}^n |M_{sim} - M_{obs}|}{n \cdot \sum_{i=1}^n M_{sim}} \times 100\%$$

In the formula, n is the number of observation points for simulating the test, M_i is the simulation value of the mode at the observation point, and O_i is the observed value of the observation point.

In addition, the model uses Nash-Sutcliffe coefficient of determination.

Table 7: Simulation and observation of the accumulated threshold model.

Parameter/Type	Simulated Accumulated Temperature (°C)	Observed Accumulated Temperature (°C)
1	103.03	146.23
2	40.02	49.76

Table 8: Model analysis and statistics test.

Indicator Type	RME	NS
Simulation Test of the Model	10.65	81.5

Coefficient of Determination

$$NS = 1 - \frac{\sum_{t=1}^T (M_t - O_t)^2}{\sum_{t=1}^T (O_t - \bar{O})^2} \times 100\%$$

Here, M_t is the simulated value of the mode at an observation point on the time sequence and O_t is the observed value at an observation point on the time sequence. Comparison of the simulated values and observed values (Table 8) shows that the simulated temperature value forecasted by the model maintained a highly consistent changing trend. The coefficient of determination was 81.5, which was greater than 65, indicating that the effect of the warning model in this research area was ideal.

ACCUMULATED TEMPERATURE DISTRIBUTION IN THE WATERSHED OF SNOWMELT FLOOD

Finally, the accumulated temperature distribution in the watershed was determined based on the grid scale with a resolution of 30 m DEM. According to relations (7) and (8) and combined with the temperature lapse rate of the altitude, the area below the zero degree contour was determined as the distribution area of the accumulated snow in the mountain, as shown in Fig. 7.

Based on the determined accumulated temperature distribution that induces snowmelt flood in the watershed, effective measures can be taken to prevent snowmelt flood. Before the significant rise in temperature, a reflective film or other reflective materials can be placed on the snowpack in the accumulated temperature distribution area to reduce the absorption of solar radiation by the snow. In addition, strengthening mountain watershed management and soil and water conservation work; returning farmland to the forest; improving the forest vegetation coverage rate in the mountain area; reducing the intensity of solar radiation; decreasing the thermal convection of the atmosphere; reducing the sediment content in the snowmelt water in the snowmelt period; and guaranteeing water quality and stability of ecological environment are necessary.

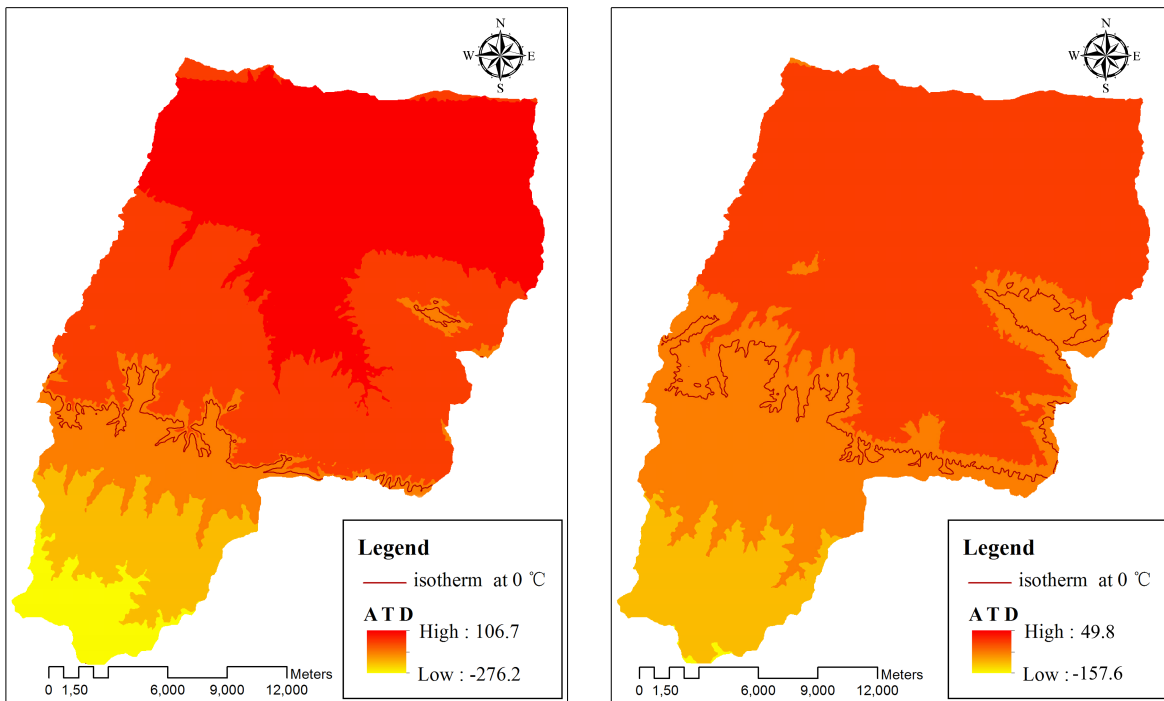


Fig. 7: Accumulated temperature distribution in the watershed of snowmelt flood.

CONCLUSION

Considering the serious influence of snowmelt flood on the ecological environment in the mountain area, an accumulated temperature distribution model under snowmelt flood warning and snowmelt flood magnitude was designed in this paper. Compared with the calculation of the forward problem, the problem solution of the model first lumps the watersheds and then makes allocation based on the magnitude response to determine the temperature distribution. The model follows the laws of energy conservation and water balance. The negative problem violates the natural order of physical process. Thus, many good properties in the positive problem are unsatisfied.

Research on the accumulated temperature distribution in the watershed of the snowmelt flood magnitude provides the decision-making basis for protecting the ecological environment and vegetation in the mountain area. In addition, planting more trees and vegetation to prevent flood and conserve water and soil; reducing the intensity of solar radiation; reducing the intensity and frequency of the snowmelt flood; improving the self-healing ability of the ecology and the vegetation coverage; cutting flood peak; reducing the amount of sand flowing into the river and debris; improving flood control and mitigation; supplementing low water flow; improving the water environment condition in the watershed; decreasing the occurrence of flood and drought disasters; and improving the ecological environment in the watershed can prevent snowmelt flood. Moreover, major sudden pollution accidents during the snowmelt flood period can be effectively prevented. Monitoring water resources, ecological pollution, and floodwater quality can provide a scientific basis for preventing the outbreak of diseases.

ACKNOWLEDGEMENTS

This research was financed by the National Natural Science

fund project of China (41171023).

REFERENCES

- Berezowski, T., Nossent, J., Chormański, J. and Batelaan, O. 2015. Spatial sensitivity analysis of snow cover data in a distributed rainfall-runoff model. *Hydrology and Earth System Sciences*, 19(4): 1887-1904.
- Blöschl, G. and Kirnbauer, R. 1991. Point snowmelt models with different degrees of complexity-internal processes. *Journal of Hydrology*, 129(1): 127-147.
- Blöschl, G., Kirnbauer, R. and Gutknecht, D. 1990. Modelling snowmelt in a mountainous river basin on an event basis. *Journal of Hydrology*, 113(1): 207-229.
- Frey, S. and Holzmann, H. 2015. A conceptual, distributed snow redistribution model. *Hydrology and Earth System Sciences Discussions*, 12(1): 609-637.
- Gautam, D. K. and Dulal, K. 2013. Determination of threshold runoff for flood early warning in Nepalese Rivers. *IDRiM Journal*, 3(1): 126-136.
- Georgakakos, K. P. and Bras, R. L. 1984. A hydrologically useful station precipitation model: 1. Formulation. *Water Resources Research*, 20(11): 1585-1596.
- Hock, R. 2003. Temperature index melt modelling in mountain areas. *Journal of Hydrology*, 282(1): 104-115.
- Kumar, A., Sarkar, S. A. and Sharma, N. 2015. Snowmelt runoff modeling in an Indian Himalayan river basin using WinSRM, RS and GIS. *Water and Energy International*, 58(1): 65-72.
- Montesarchio, V., Lombardo, F. and Napolitano, F. 2009. Rainfall thresholds and flood warning: An operative case study. *Natural Hazards and Earth System Science*, 9(1): 135-144.
- Sun, M., Yao, X., Li, Z. and Zhang, M. 2015. Hydrological processes of glacier and snow melting and runoff in the Urumqi River source region, eastern Tianshan Mountains, China. *Journal of Geographical Sciences*, 25(2): 149-164.
- Sun, Y., Hou, Z., Huang, M., Tian, F. and Ruby Leung, L. 2013. Inverse modeling of hydrologic parameters using surface flux and run off observations in the community land model. *Hydrology and Earth System Sciences*, 17(12): 4995-5011.
- Xian-yong, M., Xiao-nan, J., Zhi-hui, L., Xi, C. and Shi-feng, F. 2013. Study on snowmelt runoff under climate change effect in Tianshan Mountain in China. *Nature Environment and Pollution Technology*, 12(4): 555-562.
- Xu, Q. 2013. Retrieval method for estimating snow depth using hyperspectral data in snowmelt period. *Spectroscopy and Spectral Analysis*, 33(7): 1927-1931.